

Characterization of the New Class of Driving Cycles for Connected and Automated Vehicles

Dimitris Assanis, *Member, IEEE*, Lihui Zhao, *Member, IEEE*,
Andreas A. Malikopoulos, *Senior Member, IEEE*

Abstract—Connected and automated vehicles (CAVs) provide the most intriguing opportunity to improve traffic flow and eventually reshape the driving cycle of a typical commute. In this paper, we use a corridor consisting of a four-way intersection, a merging roadway, and a speed reduction zone to evaluate and quantify the impact of CAVs on a typical driving cycle. First, we use conventional vehicles that travel through this corridor to identify the baseline driving cycle, and then we use CAVs to determine how the baseline driving cycle is altered. We introduce specific metrics to quantitatively characterize a driving cycle and use these metrics to prescribe the new class of driving cycles for CAVs.

I. INTRODUCTION

The US Congress enacted legislation in 1975 to create the Corporate Average Fuel Economy (CAFE) standards to improve the fleet-wide vehicle fuel consumption and associated emissions of passenger vehicles and light-duty trucks. In accordance, vehicles are placed on chassis dynamometers to measure fuel economy and emissions metrics [1] during standardized driving cycles (or schedules). Such pre-determined vehicle speed profiles have been established by the US Environmental Protection Agency (EPA) and are intended to resemble both city and highway conditions.

Intersections, merging roadways, and speed reduction zones along with the driver responses to various disturbances [2] are the primary source of shaping a driving cycle in a typical commute. Connected and automated vehicles (CAVs) provide the most intriguing opportunity to improve traffic flow in such scenarios and eventually reshape the driving cycle as we know it. A connected and automated transportation system can alleviate congestion by increasing significantly traffic flow as a result of coordinating the vehicles at intersections, merging roadways, and speed reduction zones.

One of the early efforts in this direction was proposed by Dresner and Stone [3] using a reservation scheme to control a signal-free intersection of two roads. Since then, numerous approaches have been reported in the literature towards developing autonomous intersections [4]–[6]. Some approaches have focused on coordinating vehicles at intersections to improve the travel time [7]–[10]. More recently, a study [11] indicated that transitioning from intersections

This research was supported in part by ARPAE's NEXTCAR program under the award number DE-AR0000796 and in part by the US DOE Vehicle Technologies Office (VTO) under the Systems and Modeling for Accelerated Research in Transportation (SMART) Mobility Laboratory Consortium, an initiative of the Energy Efficient Mobility Systems (EEMS) Program.

The authors are with the Department of Mechanical Engineering, University of Delaware, Newark, DE 19716 USA (emails: dimitris@udel.edu; lhzhao@udel.edu; andreas@udel.edu.)

with traffic lights to signal-free intersections has the potential of doubling capacity and reducing delays. Vehicle merging is another source of bottlenecks. Ramp metering has been used to regulate the flow of vehicles at merging roadways to decrease traffic congestion [12]–[16]. Finally, speed reduction zones can also cause bottlenecks that can build up as vehicles exceed the bottleneck capacity. To address this, speed harmonization is used to provide drivers information about the appropriate speed in the upstream so as to avoid entering with high speed into the bottleneck. Thus, the speed of queue built-up decreases and the congestion recovery time is reduced [17]. A detailed discussion of the research efforts on coordination of CAVs that have been reported in the literature to date can be found in [18].

There have been efforts reported in the literature to identify and quantify fuel economy benefits of CAVs by Mersky et al. [19], Manzie et al. [20], and Hayeri et al. [21]. Liu et al. [22] quantified the impacts of coordination of CAVs on emissions. Fagnant et al. [23] and Wadud et al. [24] studied extensively the potential energy and safety impacts that CAVs might have in our society. Wu et al. [25] recommended a fuel economy optimization system that is applicable to a mixed environment of autonomous and human driven vehicles.

In earlier work, a decentralized optimal control framework was established for coordinating online CAVs to improve the efficiency in urban intersections [26]–[28], merging roadways [29], [30], roundabouts [31], speed reduction zones [17], and a corridor [32]. In this paper, we use this framework in a corridor consisting of (1) a four-way intersection, (2) a merging roadway, and (3) a speed reduction zone to evaluate and quantify the benefits of the new class of driving cycles for CAVs. First, we use conventional vehicles that travel through this corridor to identify the baseline driving cycle, and then we use CAVs at 100% penetration to determine how the baseline driving cycles is altered. We introduce specific metrics to quantitatively characterize a driving cycle and use these metrics to prescribe the new class of driving cycles.

The structure of the paper is organized as follows. In Section II, we present the simulation setup and traffic environment to prescribe the driving cycle of the corridor. In Section III, we introduce assessment metrics to characterize the driving cycle and discuss the simulation results. Finally, we draw concluding remarks in Section IV.

II. SIMULATION SETUP

The speed profiles of conventional vehicles (human-driven vehicles) and CAVs are compared on three traffic networks.

An intersection, a highway segment with an on-ramp merging section, and a highway segment with a speed reduction zone have been developed in PTV VISSIM, an appropriate software platform for simulating common traffic conditions.

The Wiedemann car following model [33], adopted in VISSIM, is used for the conventional vehicle baseline driving cycle. This model with the default parameters is selected because the minimum safe distance is defined as a function of the standstill distance (1.5 m) and headway time (1.2 sec) [34] to simulate the drivers' car following behavior.

The baseline driving cycle is altered using the decentralized optimal control framework reported in [17], [27], [30], in which a *control zone* is defined before the conflict area, i.e., the region at the center of the intersection, merging point, or the start of the speed reduction zone. A unique identifying number is assigned to a CAV when it enters the control zone and an appropriate time to pass through the conflict area is determined so as to avoid any possible collisions with other vehicles.

A desired headway time (1.2 sec) similar to human-driven vehicles is used for the CAVs to avoid collisions. The total simulation duration (3600 sec) has a resolution of 10 time steps per second. Detailed traffic information and simulation setup are described in the following sections by network.

A. Intersection

We consider a four-leg intersection in Newark, Delaware area (Fig. 1) with a one-lane roadway for westbound traffic and two-lane roadway for the other directional traffic. Dedicated left-turn and/or right-turn lanes exist for each direction to accommodate turning traffic. The average annual daily traffic counts for the intersection [35] is applied and set as part of the base traffic inputs. We take 25%, 50%, and 100% of the traffic volume to reflect light, medium, and heavy traffic conditions and optimize the signal timing for the intersection, respectively, assuming that a fixed-time signal controller is present for the intersection with a 60-sec cycle time. Note that although we are not considering an actuated signal controller, the fixed time is optimal for the imposed traffic conditions. For the base traffic volume, we adopt an extension to the 120-sec cycle time due to the extreme delay for the northbound and southbound traffic. The speed limit is set as 55 *kph*. The length of the road in each direction of the intersection is approximately 1100 *m*, and the intersection is located approximately 500 *m* from each entry point. The length of the control zone is 250 *m*.

B. Merging Roadway

We consider a two-lane highway segment (Fig. 2) with an one-lane on-ramp. We apply a higher speed limit of 85 *kph* to reflect highway traffic conditions. The merging point is located 400 *m* downstream of the entry points on both mainline highway and the ramp. The length of the control zone is 250 *m*. For human-driven vehicles without coordination, the vehicles traveling on the ramp need to yield to vehicles traveling on the primary road, or perhaps even stop and wait for an appropriate gap to merge into

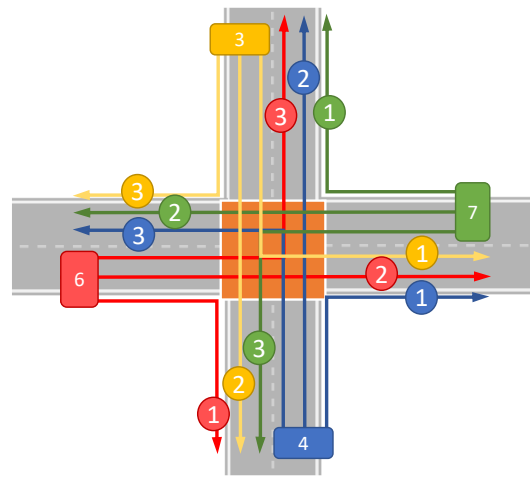


Fig. 1. A four-way intersection with twelve possible trajectories.

the mainline highway flow. On the contrary, CAVs on the primary road and ramp are able to cooperate with each other to create appropriate gaps, such that the traffic flow is improved substantially for the overall network.

Under light traffic conditions, we set 1200 vehicles per hour (*vph*) and 600 *vph* traffic volumes for the mainline highway and the ramp respectively. An increase to 2000 *vph* and 2800 *vph* for mainline traffic is considered as medium and high traffic demand situation respectively.

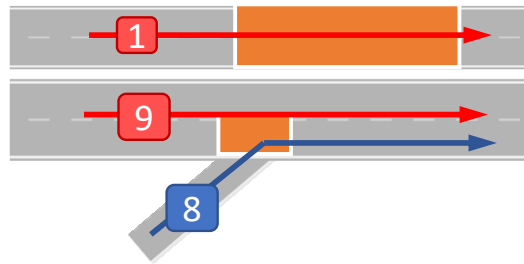


Fig. 2. Top: A speed reduction zone with a singular trajectory. Bottom: A merging roadway with two possible trajectories.

C. Speed Reduction Zone

A two-lane highway segment (1200 *m* total length) (Fig. 2) is outfitted with a 20 *kph* speed reduction zone (200 *m* length) causing typical congestion that propagates upstream. The entry and downstream speed limits for the zone are 65 *kph* and 85 *kph* respectively. Due to large speed drop, the length of the control zone is set to be 350 *m* to ensure smooth controlled traffic flow. We apply 1200 *vph* to reflect light traffic volume, 2000 *vph* for the medium traffic volume, and 2800 *vph* for the high traffic volume.

III. SIMULATION RESULTS & DISCUSSION

A. Driving Cycle Along Corridor

The baseline and CAV driving cycles are determined through multiple numerical simulations of vehicles navigating a corridor, formed of the three traffic networks described

above at three varying traffic volumes (low, medium, and high). Representative driving cycles are shown in Fig. 3 and Fig. 4 through speed time histories of vehicles with similar routing in the four way intersection, specifically traveling in the southbound direction and heading straight.

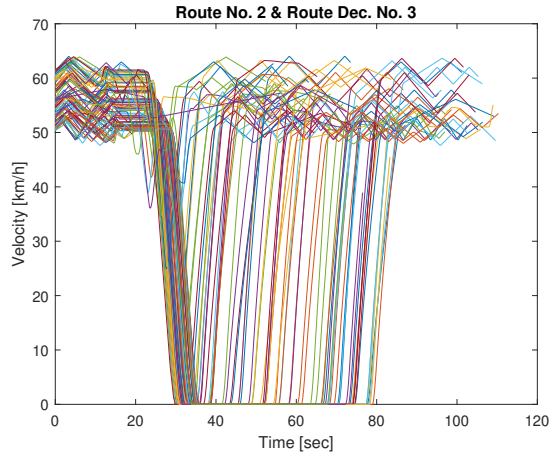


Fig. 3. Conventional vehicle driving cycles through an intersection.

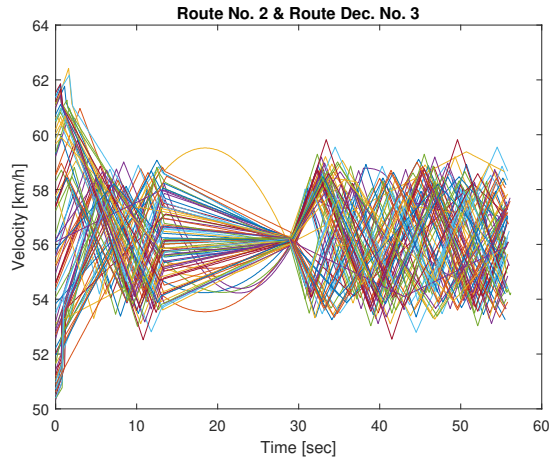


Fig. 4. CAV driving cycles through an intersection.

Conventional vehicles are forced to come to a full stop and wait for the traffic light to change (Fig. 3) while CAVs are optimally coordinated through a signal-free intersection and never come to a stand still throughout the intersection (Fig. 4), decreasing the overall travel time from just over 100 *sec* to approximately 55 *sec*. Vehicles enter the control zone approximately 12 *sec* into the route evaluation and exit at approximately 30 *sec*, where an inflection point is observed marking the end of the control zone and the beginning of the intersection. There is less than 10% variation in vehicle speed during the coordination which far exceeds the undesirable standstill conditions experienced by conventional vehicles on a signaled network.

B. Assessment Metrics

Similarly routed baseline and controlled vehicle speed time histories are comparatively evaluated to determine key

performance metrics. The speed time histories of interest spanning the distance from the start of the control zone to the end of the intersection will be the focus of this comparative study. Malikopoulos and Aguilar [2] proposed two relevant metrics, the stop factor and the coefficient of power demand, to quantify the impact on fuel consumption and associated generated emissions. These two metrics are described below. The comparative and quantitative evaluation of the generated drive cycles are assessed based on these metrics as well as the travel time which is computed as follows

$$t_{travel} = \int_0^{x_{end}} t(x) \cdot dx = t(x) \Big|_{x=x_{end}} - t(x) \Big|_{x=0} \quad (1)$$

where t_{travel} is the time the vehicle travels from the starting point of the driving cycle, $x = 0$, to the end x_{end} . The total time that the vehicle speed $v(t)$ is zero can be computed as follows

$$t_{stop} = \sum t \Big|_{v(t)=0} \quad (2)$$

The stop factor, f_{stop} , [2] is the percentage of stopped time, t_{stop} , the vehicle experiences during the total travel time, t_{end}

$$f_{stop} = \frac{t_{stop}}{t_{end}} \cdot 100. \quad (3)$$

The power, P , is the rate quantity of doing work, W , per unit time, t . Work is equivalent to a force, F applied over a distance d . Reorganizing the equation, Force is equivalent to the mass, m of the vehicle times the acceleration, a , of the vehicle. Namely,

$$P = \frac{W}{t} = \frac{(F \cdot d)}{t} = F \cdot \frac{d}{t} = (m \cdot a) \cdot \frac{d}{t} = m \cdot a \cdot v(t). \quad (4)$$

The coefficient of power demand [2] is the product $a \cdot v(t)$ and provides an indication of the transient engine operation [36], [37] since it is proportional to power demanded by the driver (4). For traffic networks with multiple routes, i.e. four-way intersection, each route generates one temporally averaged value per assessment metric. This can be further cumulatively reported as a singular value as the average of route averaged values with one standard deviation of the route averaged values to reflect the variation along the different routes.

C. Intersection

For the four-way intersection, a vehicle can travel 12 possible routes (Fig. 1), along the four cardinal directions, Northbound (NB), Eastbound (EB), Southbound (SB), or westbound (WB), a vehicle can make any of following three route decisions: left turn (LT), straight (ST), or right turn (RT). We analyzed a total of 700, 1500, and 3300 cars for the low, medium, and high traffic volume cases, respectively.

Further analyzing the vehicle speed trajectories by route, the ensemble average of all vehicle on a particular route and corresponding to a particular volume are shown in Fig. 5. It is extremely evident that the average travel time is significantly reduced by the signal-free controlled CAVs.

The average change in travel time for all routes at the four-way intersection was determined to be $-24.4 \pm 22.5\%$, $-35.9 \pm 23.1\%$, and $-45.9 \pm 21.6\%$ for low, medium, and high traffic volumes, respectively. The controlled CAVs were able to completely eliminate all stoppage time along the route for all traffic conditions (Fig. 6).

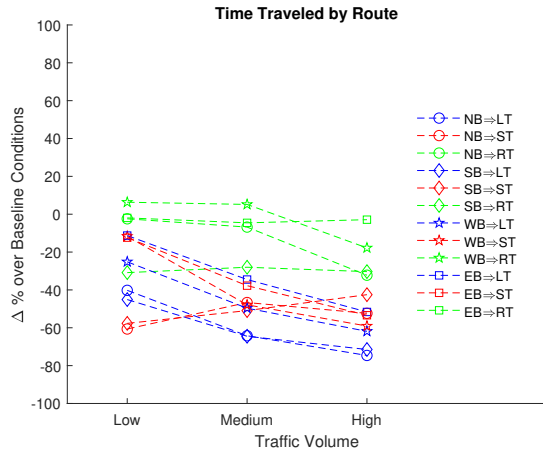


Fig. 5. Travel time by intersection route for varying traffic volumes.

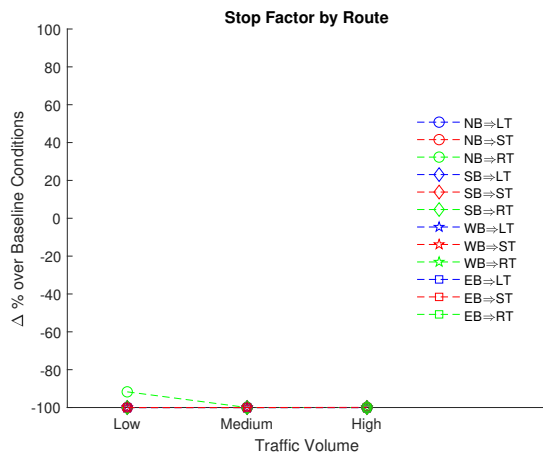


Fig. 6. Stop factor by intersection route for varying traffic volumes.

The average change in vehicle speed by route (Fig. 7), is determined as $-31.8 \pm 40.2\%$, $45.2 \pm 40.1\%$, and $66.4 \pm 58.3\%$ for low, medium, and high traffic volumes, respectively. The average change in the coefficient of power demand by route (Fig. 8), is determined as $-83.4 \pm 9.0\%$, $-82.1 \pm 10.1\%$, and $-74.5 \pm 8.9\%$ for low, medium, and high traffic volumes, respectively.

D. Merging Roadway

The merging roadway has a total of two possible routes, the mainline route proceeding straight or the ramp route merging into the mainline (Fig. 2). We analyzed a total of 1200, 2000, and 2550 cars for the low, medium, and high traffic volume cases, respectively.

The average change in travel time (Fig. 9), for a vehicle merging from the ramp on to the mainline, is determined

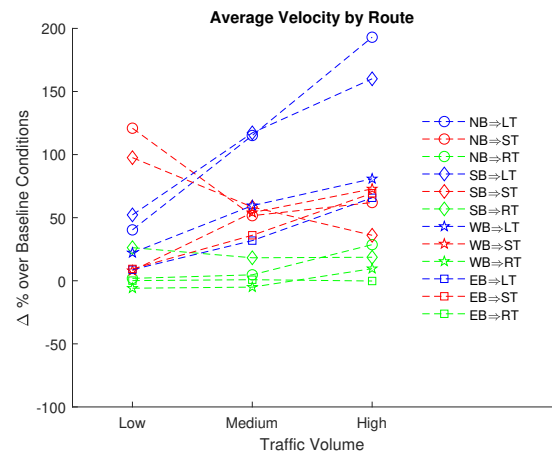


Fig. 7. Average speed by intersection route for varying traffic volumes.

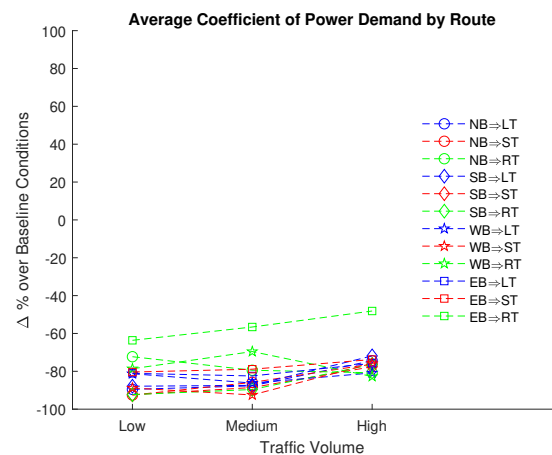


Fig. 8. Average coefficient of power demanded by intersection route for varying traffic volumes.

as -16.6% , -35.9% , and -89.7% for low, medium, and high traffic volumes, respectively. The average travel time did not change for vehicles on the mainline route regardless of traffic volume studied. Controlled CAVs merging from the ramp on to the mainline route are able to completely eliminate all stoppage time along the route for all traffic conditions (Fig. 10).

The merging vehicle change in average speed (Fig. 11), is determined as 15.2% , 40.2% , and 513.4% for low, medium, and high traffic volumes, respectively. The average change in speed for a vehicle on the mainline remains virtually unchanged for different traffic volumes.

The average change in coefficient of power demand by route for a merging vehicle (Fig. 12), is determined as -93.0% , -89.0% , and -72.5% for low, medium, and high traffic volumes, respectively. The average change in coefficient of power demand by route for a vehicle on the mainline is determined as -15.3% , -18.1% , and -10.1% for low, medium, and high traffic volumes, respectively.

E. Speed Reduction Zone

The speed reduction zone traffic network has only one possible route for the vehicles to travel (Fig. 2). We analyzed

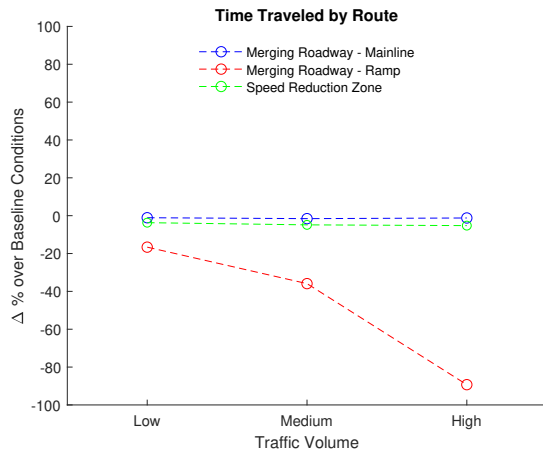


Fig. 9. Average travel time of traffic networks at varying traffic volumes.

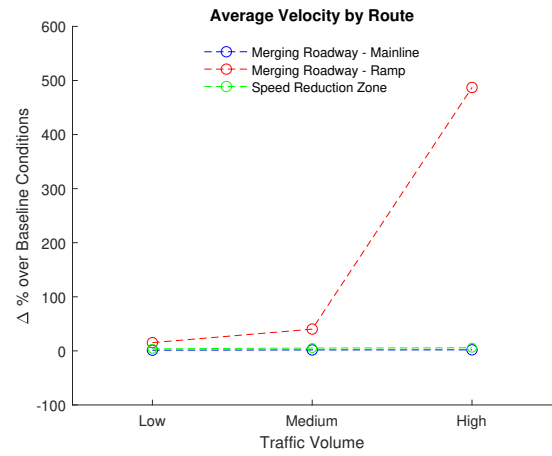


Fig. 11. Average speed of traffic networks at varying traffic volumes.

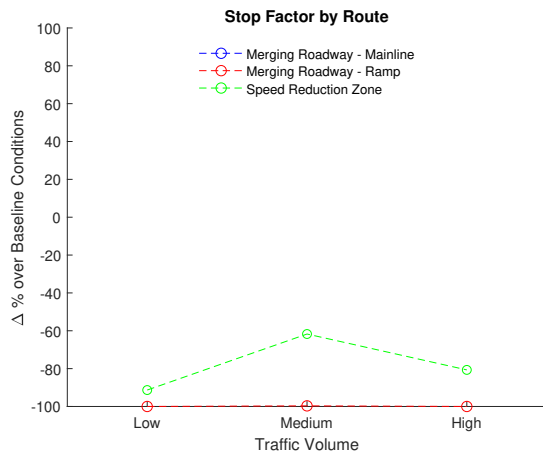


Fig. 10. Stop factor of traffic networks at varying traffic volumes.

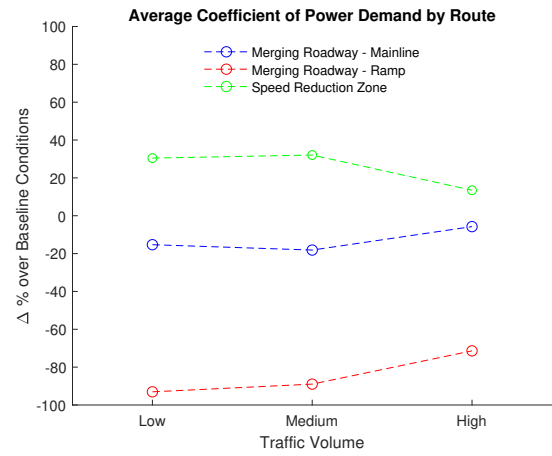


Fig. 12. Power demanded of traffic networks at varying traffic volumes.

a total of 700, 1250, and 2000 cars for the low, medium, and high traffic volume cases, respectively.

The average change in travel time (Fig. 9), for a vehicle in the speed reduction zone is determined as -3.7%, -4.9%, and -5.3% for low, medium, and high traffic volumes, respectively. The stop factor for the speed reduction zone is modified from tracking stand-still conditions to tracking velocities that are less than 18 *kph*, 10% less than the imposed speed limit of 20 *kph*. The average change in the stop factor for controlled CAVs, compared to conventional vehicles, in the speed reduction zone (Fig. 10), is determined as -91.3%, -61.2%, and -80.1% for low, medium, and high traffic volumes, respectively.

The average change in vehicle speed in a speed reduction zone (Fig. 11), is determined as 3.8%, 5.2%, and 5.7% for low, medium, and high traffic volumes, respectively. The average change in coefficient of power demand in a speed reduction zone (Fig. 12), is determined as 30.5%, 32.1%, and 13.5% for low, medium, and high traffic volumes, respectively. The increase in coefficient of power demanded is counter to the our expectations. We believe the traffic volumes selected needs to be increased for the speed reduction zone coordination to highlight the improvement in travel time

and power demanded.

IV. CONCLUDING REMARKS

The results presented in this paper aim at evaluating and quantifying the differences between conventional vehicles and CAVs along a corridor consisting of a four-way intersection, a merging roadway, and a speed reduction zone. We note that coordination of CAVs can decrease the fleet average travel time in the three traffic networks studied at varying traffic volumes meaning that individuals can arrive at their destination sooner. We also observe that coordination of CAVs can increase the fleet average speed in all three traffic networks and at all varying traffic volumes meaning that the infrastructure throughput capacity is effectively increased. Coordination of CAVs can virtually eliminate all stand-still traffic conditions, greatly improving a critical bottleneck in a transportation network. Ultimately, we can decrease overall fleet power demand, thus paving the way for an improvement in the overall fleet fuel efficiency and a decrease in resulting emissions generated. The improvement in traffic flow is achieved by removing the driver out of the driving equation and thus reshaping the driving cycle of the typical commute.

These landmark results highlight the significant potential

impacts that coordination enabled by CAVs can have over conventional vehicles. Great potential for fuel economy savings and corresponding decrease in emissions generation exists for the coordination of CAVs on the three traffic networks of a four-way intersection, a merging roadway, and a speed reduction zone at different traffic volumes.

Future work should further focus on the qualification of more detailed energy consumption and emission generation of CAVs. Different roadway infrastructure such as roundabouts and complex, compound intersections should also be investigated. Additional efforts should be focused on further refining possible drive cycle tests and metrics to be used to analyze and benchmark CAV performance.

REFERENCES

- [1] U.S. E.P.A., "Passenger Car Fuel Economy - Dynamometer vs. Track vs. Road," Tech. Rep., 1975.
- [2] A. A. Malikopoulos and J. P. Aguilar, "An Optimization Framework for Driver Feedback Systems," *IEEE Transactions on Intelligent Transportation Systems*, vol. 14, no. 2, pp. 955–964, 2013.
- [3] K. Dresner and P. Stone, "Multiagent traffic management: a reservation-based intersection control mechanism," in *Proceedings of the Third International Joint Conference on Autonomous Agents and Multiagents Systems*, 2004, pp. 530–537.
- [4] K. Dresner and P. Stone, "A Multiagent Approach to Autonomous Intersection Management," *Journal of Artificial Intelligence Research*, vol. 31, pp. 591–653, 2008.
- [5] A. de La Fortelle, "Analysis of reservation algorithms for cooperative planning at intersections," *13th International IEEE Conference on Intelligent Transportation Systems*, pp. 445–449, Sept. 2010.
- [6] S. Huang, A. Sadek, and Y. Zhao, "Assessing the Mobility and Environmental Benefits of Reservation-Based Intelligent Intersections Using an Integrated Simulator," *IEEE Transactions on Intelligent Transportation Systems*, vol. 13, no. 3, pp. 1201,1214, 2012.
- [7] I. H. Zohdy, R. K. Kamalanathsharma, and H. Rakha, "Intersection management for autonomous vehicles using iCACC," *2012 15th International IEEE Conference on Intelligent Transportation Systems*, pp. 1109–1114, 2012.
- [8] F. Yan, M. Dridi, and A. El Moudni, "Autonomous vehicle sequencing algorithm at isolated intersections," *2009 12th International IEEE Conference on Intelligent Transportation Systems*, pp. 1–6, 2009.
- [9] J. Lee, B. B. Park, K. Malakorn, and J. J. So, "Sustainability assessments of cooperative vehicle intersection control at an urban corridor," *Transportation Research Part C: Emerging Technologies*, vol. 32, pp. 193–206, 2013.
- [10] F. Zhu and S. V. Ukkusuri, "A linear programming formulation for autonomous intersection control within a dynamic traffic assignment and connected vehicle environment," *Transportation Research Part C: Emerging Technologies*, Jan. 2015.
- [11] R. Tachet, P. Santi, S. Sobolevsky, L. I. Reyes-Castro, E. Frazzoli, D. Helbing, and C. Ratti, "Revisiting street intersections using slot-based systems," *PLOS ONE*, vol. 11, no. 3, 2016.
- [12] M. Papageorgiou, H. Hadj-Salem, and J.-M. Blouffeville, "ALINEA: A local feedback control law for on-ramp metering," *Transportation Research Record 1320*, 1991.
- [13] M. Papageorgiou and A. Kotsialos, "Freeway Ramp Metering: An Overview," *IEEE Transactions on Intelligent Transportation Systems*, vol. 3, no. 4, pp. 271–281, 2002.
- [14] I. Papamichail and M. Papageorgiou, "Traffic-Responsive Linked Ramp-Metering Control," *IEEE Transactions on Intelligent Transportation Systems*, vol. 9, no. 1, pp. 111–121, 2008.
- [15] R. C. Carlson, I. Papamichail, and M. Papageorgiou, "Local feedback-based mainstream traffic flow control on motorways using variable speed limits," *IEEE Transactions on Intelligent Transportation Systems*, vol. 12, no. 4, pp. 1261–1276, 2011.
- [16] G.-R. Iordanidou, C. Roncoli, I. Papamichail, and M. Papageorgiou, "Feedback-Based Mainstream Traffic Flow Control for Multiple Bottlenecks on Motorways," *IEEE Transactions on Intelligent Transportation Systems*, pp. 1–12, 2014.
- [17] A. A. Malikopoulos, S. Hong, B. Park, J. Lee, and S. Ryu, "Optimal control for speed harmonization of automated vehicles," *IEEE Transactions on Intelligent Transportation Systems*, 2018 (in press).
- [18] J. Rios-Torres and A. A. Malikopoulos, "A Survey on Coordination of Connected and Automated Vehicles at Intersections and Merging at Highway On-Ramps," *IEEE Transactions on Intelligent Transportation Systems*, vol. 18, no. 5, pp. 1066–1077, 2017.
- [19] A. C. Mersky and C. Samaras, "Fuel economy testing of autonomous vehicles," *Transportation Research Part C: Emerging Technologies*, vol. 65, pp. 31–48, 2016. [Online]. Available: <http://dx.doi.org/10.1016/j.trc.2016.01.001>
- [20] C. Manzie, H. Watson, and S. Halgamuge, "Fuel economy improvements for urban driving: Hybrid vs. intelligent vehicles," *Transportation Research Part C: Emerging Technologies*, vol. 15, no. 1, pp. 1–16, 2007.
- [21] S. Vasebi, Y. M. Hayeri, C. Samaras, and C. Hendrickson, "Low-level automated light-duty vehicle technologies provide opportunities to reduce fuel consumption," in *Transportation Research Board 97th Annual Meeting*, 2018.
- [22] J. Liu, K. Kockelman, and A. Nichols, "Anticipating the emissions impacts of smoother driving by connected and autonomous vehicles, using the moves model," in *Transportation Research Board 96th Annual Meeting*, 2017.
- [23] D. J. Fagnant and K. Kockelman, "Preparing a nation for autonomous vehicles: Opportunities, barriers and policy recommendations," *Transportation Research Part A: Policy and Practice*, vol. 77, pp. 167–181, 2015.
- [24] Z. Wadud, D. MacKenzie, and P. Leiby, "Help or hindrance? The travel, energy and carbon impacts of highly automated vehicles," *Transportation Research Part A: Policy and Practice*, vol. 86, pp. 1–18, 2016.
- [25] C. Wu, G. Zhao, and B. Ou, "A fuel economy optimization system with applications in vehicles with human drivers and autonomous vehicles," *Transportation Research Part D: Transport and Environment*, vol. 16, no. 7, pp. 515–524, 2011.
- [26] Y. Zhang, A. A. Malikopoulos, and C. G. Cassandras, "Optimal control and coordination of connected and automated vehicles at urban traffic intersections," in *Proceedings of the American Control Conference*, 2016, pp. 6227–6232.
- [27] A. A. Malikopoulos, C. G. Cassandras, and Y. J. Zhang, "A decentralized energy-optimal control framework for connected automated vehicles at signal-free intersections," *Automatica*, vol. 93, pp. 244 – 256, 2018.
- [28] A. Stager, L. Bhan, A. A. Malikopoulos, and L. Zhao, "A scaled smart city for experimental validation of connected and automated vehicles," in *15th IFAC Symposium on Control in Transportation Systems*, 2018, pp. 120–135.
- [29] J. Rios-Torres, A. A. Malikopoulos, and P. Pisu, "Online Optimal Control of Connected Vehicles for Efficient Traffic Flow at Merging Roads," in *2015 IEEE 18th International Conference on Intelligent Transportation Systems*, 2015, pp. 2432–2437.
- [30] J. Rios-Torres and A. A. Malikopoulos, "Automated and Cooperative Vehicle Merging at Highway On-Ramps," *IEEE Transactions on Intelligent Transportation Systems*, vol. 18, no. 4, pp. 780–789, 2017.
- [31] L. Zhao, A. A. Malikopoulos, and J. Rios-Torres, "Optimal control of connected and automated vehicles at roundabouts: An investigation in a mixed-traffic environment," in *15th IFAC Symposium on Control in Transportation Systems*, 2018, pp. 73–78.
- [32] L. Zhao and A. A. Malikopoulos, "Decentralized optimal control of connected and automated vehicles in a corridor," in *2018 IEEE 21th International Conference on Intelligent Transportation Systems*, 2018.
- [33] R. Wiedemann, "Simulation des Strassenverkehrsflusses," Institut für Verkehrswesen der Universität Karlsruhe, UC Berkeley Transportation Library - Accession Number: 00896074, 1974.
- [34] P. Group *et al.*, "Ptv vissim 7 user manual," *Germany: PTV GROUP*, 2014.
- [35] "Traffic Counts 2016 — State of Delaware." [Online]. Available: <http://opendata.firstmap.delaware.gov/datasets/traffic-counts-2016>
- [36] A. A. Malikopoulos, D. N. Assanis, and P. Y. Papalambros, "Optimal engine calibration for individual driving styles," in *SAE Proceedings, Technical Paper 2008-01-1367*, 2008.
- [37] A. A. Malikopoulos, P. Y. Papalambros, and D. N. Assanis, "Online identification and stochastic control for autonomous internal combustion engines," *Journal of Dynamic Systems, Measurement, and Control*, vol. 132, no. 2, pp. 024 504–024 504, 2010.